Archival Report

Biological Psychiatry: Celebrating 50 Years

MicroRNA-26a/Death-Associated Protein Kinase 1 Signaling Induces Synucleinopathy and Dopaminergic Neuron Degeneration in Parkinson's Disease

Ying Su, Man-Fei Deng, Wan Xiong, Ao-Ji Xie, Jifeng Guo, Zhi-Hou Liang, Bo Hu, Jian-Guo Chen, Xiongwei Zhu, Heng-Ye Man, Youming Lu, Dan Liu, Beisha Tang, and Ling-Qiang Zhu

ABSTRACT

BACKGROUND: Death-associated protein kinase 1 (DAPK1) is a widely distributed serine/threonine kinase that is critical for cell death in multiple neurological disorders, including Alzheimer's disease and stroke. However, little is known about the role of DAPK1 in the pathogenesis of Parkinson's disease (PD), the second most common neurodegenerative disorder.

METHODS: We used Western blot and immunohistochemistry to evaluate the alteration of DAPK1. Quantitative polymerase chain reaction and fluorescence in situ hybridization were used to analyze the expression of microRNAs in PD mice and patients with PD. Rotarod, open field, and pole tests were used to evaluate the locomotor ability. Immunofluorescence, Western blot, and filter traps were used to evaluate synucleinopathy in PD mice.

RESULTS: We found that DAPK1 is posttranscriptionally upregulated by a reduction in microRNA-26a (miR-26a) caused by a loss of the transcription factor CCAAT enhancer-binding protein alpha. The overexpression of DAPK1 in PD mice is positively correlated with neuronal synucleinopathy. Suppressing miR-26a or upregulating DAPK1 results in synucleinopathy, dopaminergic neuron cell death, and motor disabilities in wild-type mice. In contrast, genetic deletion of DAPK1 in dopaminergic neurons by crossing DAT-Cre mice with DAPK1 floxed mice effectively rescues the abnormalities in mice with chronic MPTP treatment. We further showed that DAPK1 overexpression promotes PD-like phenotypes by direct phosphorylation of α-synuclein at the serine 129 site. Correspondingly, a cell-permeable competing peptide that blocks the phosphorylation of α-synuclein prevents motor disorders, synucleinopathy, and dopaminergic neuron loss in the MPTP mice.

CONCLUSIONS: miR-26a/DAPK1 signaling cascades are essential in the formation of the molecular and cellular pathologies in PD.

Keywords: α-Synuclein, DAPK1, miRNA, MPTP, Parkinson's disease, Peptide

https://doi.org/10.1016/j.biopsych.2018.12.008

Parkinson's disease (PD) is the second most common neurodegenerative disease in people over 60 years old. In 2015, PD affected 6.2 million people and resulted in approximately 117,400 deaths globally (1). The most prominent clinical manifestations in PD are the motor symptoms, such as tremor, slowed movement (bradykinesia), rigidity, and postural instability (2), which result from the chronic loss of dopaminergic (DA) neurons in the basal ganglia, mainly in the substantia nigra (SN) (3). Pathologically, PD is also characterized by the presence of Lewy bodies and Lewy neurites, which consist of cytoplasmic inclusions of aggregated α-synuclein in a hyperphosphorylated state (4).

Death-associated protein kinase 1 (DAPK1) belongs to a family of five serine/threonine (Ser/Thr) kinases and is regulated by calcium/calmodulin (5). DAPK1 was originally shown to be essential for interferon gamma–induced cell death in HeLa cells (6), and it is considered a positive mediator of apoptosis. Both internal and external apoptotic stimulants lead to activation of DAPK1, which in turn participates in both type I apoptotic (caspase-dependent) cell death and type II autophagic (caspase-independent) cell death (7). Overexpression of exogenous DAPK1 in cell cultures results in pronounced death-associated cellular changes (8). DAPK1 is also abundant in the brain and has been reported to play important roles in neural development and multiple neurological diseases. Importantly, activated DAPK1 directly binds to and phosphorylates the *N*-methyl-D-aspartate receptor GluN2B subunit at Ser1303, which is implicated in the excitotoxicity in ischemic stroke via upregulating NR1/NR2B receptor channel conductance at the extrasynaptic sites (9). Moreover, activated

ISSN: 0006-3223

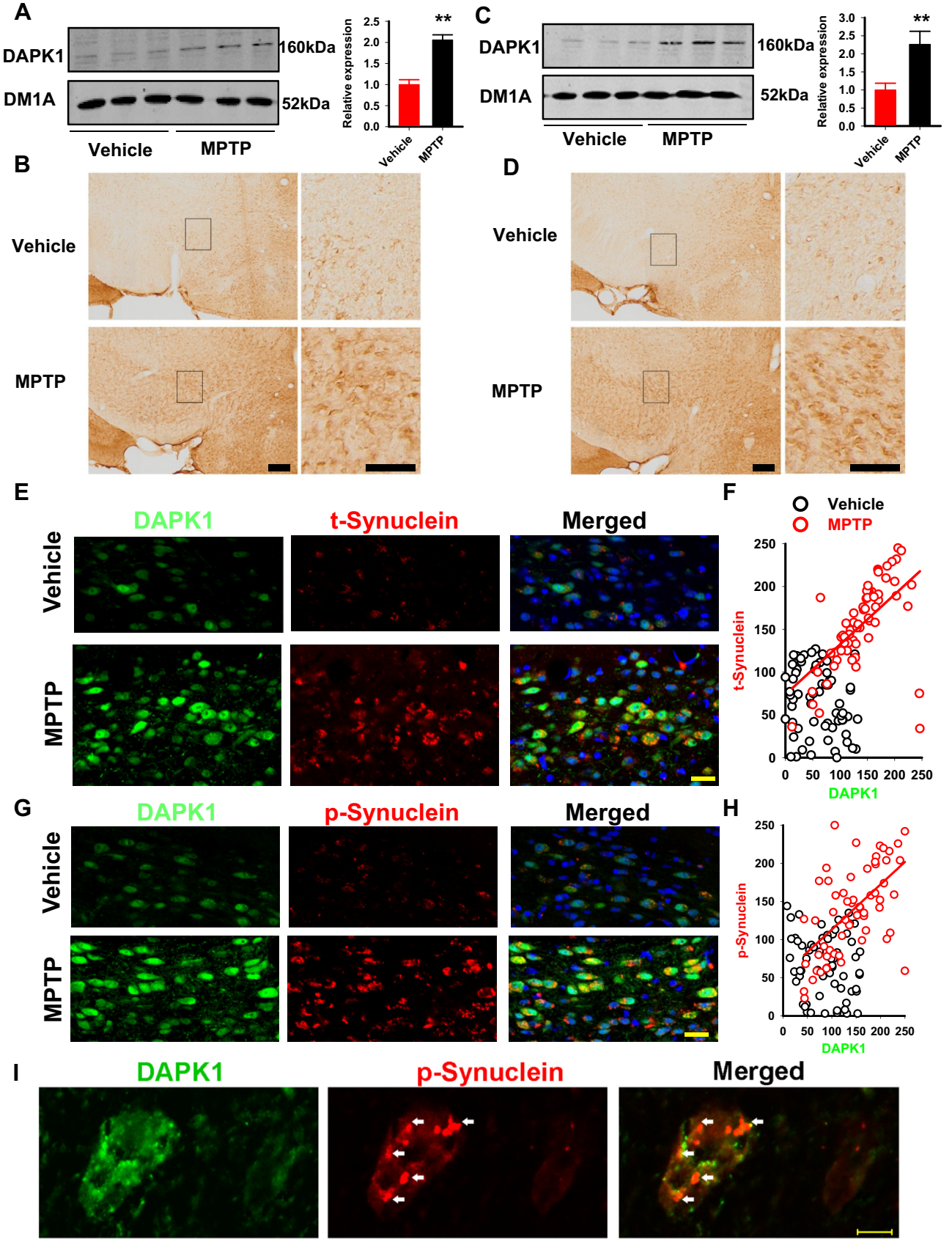
A
DAPK1
160kDa
DM1A
52kDa
Vehicle
MPTP
Relative expression
**
C
B
D
E
DAPK1
t-Synuclein
Merged
F
t-Synuclein
G
p-Synuclein
H
I

DAPK1 directly phosphorylates p53 at Ser23 and induces necrotic and apoptotic neuronal death in stroke (10). In Alzheimer's disease (AD), hippocampal DAPK1 expression is markedly increased, which enhances tau protein stability via phosphorylation at multiple AD-related sites to mediate the pathological toxicity of tau (11). However, whether the expression of DAPK1 in PD is dysregulated and how it is involved in the death of DA neurons remain unclear.

In the current study, we found that in the brain of 1-methyl-4-phenyl-1,2,3,6-tetrahydropyridine (MPTP)-induced PD mice, the protein amounts but not the messenger RNA (mRNA) levels of DAPK1 were increased. We showed that inhibition of microRNA-26a (miR-26a) caused by suppression of the transcription factor CCAAT enhancer-binding protein alpha (C/EBPα) was responsible for DAPK1 upregulation in PD mice and patients with PD. Downregulation of miR-26a and upregulation of DAPK1 induced synucleinopathy and cell death of DA neurons in vivo. DAPK1 induces synucleinopathy by direct phosphorylation of α-synuclein at the Ser129 site. Genetic deletion of DAPK1 in DA neurons rescued synucleinopathy in two PD mouse models. Furthermore, the loss of DA neurons and the locomotor deficits can also be reversed by DAPK1 deletion in mice of chronic MPTP treatment. Finally, generation of a membrane-permeable peptide to directly disrupt the association of DAPK1 and α-synuclein ameliorated both the pathological and behavioral abnormalities in the MPTP mice. Thus, our findings provide a promising novel strategy for the therapeutic intervention of PD.

METHODS AND MATERIALS

Animals

Adult male C57BL/6 mice were purchased from the National Resource Center of Model Mice (Nanjing, China). The mice with DA neuron–specific knockdown of DAPK1 were generated by crossing DAPK1-KD$^{loxp/loxp}$ transgenic mice and DAT-cre mice (No. 006660; Jackson Laboratory, Bar Harbor, ME). The M83 transgenic mice expressing the mutant human A53T α-synuclein were purchased from the Jackson Laboratory (No. 004479). All the mice were housed under a 12-hour light/dark cycle in a temperature-controlled room (22–24°C) with free access to food and water. All the experimental procedures were approved by the Institutional Animal Care and Use Committee of the Huazhong University of Science and Technology and followed American Association for Laboratory Animal Care, Division of Laboratory Animal Resources, Animal Research: Reporting of In Vivo Experiments, and National Institutes of Health animal care guidelines on Institutional Animal Care and Use Committee approved protocols.

Generation of a Highly Infectious Virus and the Mimics/Antagomirs

Mmu-miR-26a-5p mimics and the scrambled control were purchased from RiboBio (Guangzhou, China) (Supplemental Table S2). The mimics and antagomirs to upregulate/downregulate the level of miR-26a were used as previously reported (12). The AAV2/9-DAPK1 (1×10^{13} viral genomes/mL) was purchased from Allabio Technology (Shanghai, China). We injected the particles (1.5 μL at 0.2 μL/min) into each side of the SN (3.0 mm posterior to bregma; 1.0 mm lateral to midline; 4.3 mm below the dura). In this study, 28 days after the virus injection, mice were used for the phenotyping assays, including miR, mRNA, and protein expression assays, and for the behavioral tests.

Fluorescence In Situ Hybridization

Multiplexed microRNA (miRNA) fluorescence in situ hybridization is an advanced method for visualizing differentially expressed miRNAs together with other reference RNAs in fresh-frozen and archival tissues. Probes were purchased from TSINGKE (Wuhan, China) (Supplemental Table S2). For in situ hybridization in frozen brain slices, mice were perfused with 1× phosphate-buffered saline (PBS) and 4% (v/v) paraformaldehyde solution in PBS. The brain tissues were fixed in 4% (v/v) paraformaldehyde solution in PBS overnight at 4°C and subsequently cryoprotected in 30% (w/v) sucrose in PBS (diethyl pyrocarbonate treated) overnight at 4°C and cryosectioned at 16 μm thickness. The manufacturer's protocol was applied with in situ hybridization, skipping the dehydration/rehydration and proteinase QS treatment steps. Probes were diluted to 1:50. After completion of the in situ hybridization, brain slices were blocked for 1 hour in blocking buffer for immunostaining. The slices were stained overnight at 4°C using primary antibodies, washed three times with 1× PBS, and incubated with secondary antibody for 1 hour at room temperature. 4′,6-Diamidino-2-phenylindole (DAPI) was added to one of the following three washing steps with 1× PBS to visualize nuclei. Slices were then mounted for microscopy (13).

Figure 1. Death-associated protein kinase 1 (DAPK1) is increased in the 1-methyl-4-phenyl-1,2,3,6-tetrahydropyridine (MPTP) mice and is positively correlated with synucleinopathy. **(A, C)** Lysates from the substantia nigra of acute **(A)** and chronic **(C)** MPTP mice were examined by Western blot with anti-DAPK1 and anti-α-tubulin (DM1A) antibodies. Representative images are shown. The quantitative analysis was performed with Student's *t* test. $^{**}p < .01$ vs. vehicle-injected mice; $n = 3$ independent experiments by using 6 mice per group. **(B, D)** Immunohistochemical staining with anti-DAPK1 was performed in coronal slices from the acute **(B)** and chronic **(D)** MPTP-injected mice. The black rectangle regions in the left panels are shown in higher magnification in the right panels. Bar = 50 μm; Student's *t* test; $n = 3$ independent experiments by using 6 mice per group. **(E, F)** Double immunofluorescence was performed in coronal slices from the chronic MPTP-injected mice by using the DAPK1 (green) and total α-synuclein (t-Synuclein) (red) antibodies **(E)**, and the correlation analysis **(F)** was performed via SigmaPlot after the fluorescent intensity measurements were acquired via the ImageJ program. Bar = 50 μm; red and black circles are the fluorescent intensities from the MPTP- and vehicle-treated mice, respectively; $R^2 = .3401$; $p < .001$. **(G, H)** Double immunofluorescence staining was performed in coronal slices from the chronic MPTP-injected mice using DAPK1 (green) and phospho-Ser129-α-synuclein (p-Synuclein) (red) antibodies **(G)**, and the correlation analysis **(H)** was performed via SigmaPlot after the fluorescent intensity measurements were acquired via ImageJ. Bar = 50 μm; red and black circles are the fluorescent intensities from MPTP- and vehicle-treated mice, respectively; $R^2 = .3728$; $p < .001$. **(I)** Neurons with high magnification showing α-synuclein (red) inclusions (white arrow) and strong DAPK1 staining (green). The cell on the left side displays more intense DAPK1 staining. Scale bar = 10 μm.

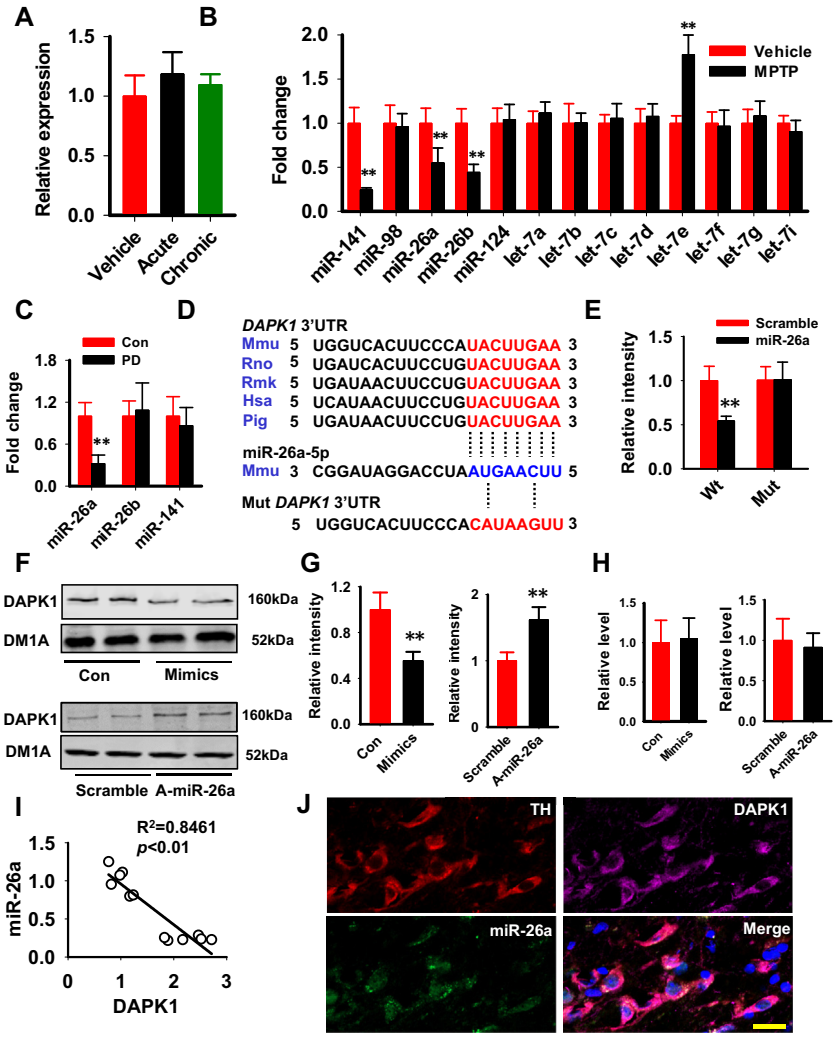

Figure 2. Abnormal downregulation of microRNA-26 (miR-26) is responsible for death-associated protein kinase 1 (DAPK1) elevation in Parkinson's disease (PD). **(A)** DAPK1 messenger RNA expression showed no change in the 1-methyl-4-phenyl-1,2,3,6-tetrahydropyridine (MPTP) models. **(B)** Alterations in predicted microRNAs that target DAPK1 in the substantia nigra of chronic MPTP-injected mice models. $^{**}p < .01$ vs. vehicle; Student's *t* test; $n = 8$ from 3 independent experiments. **(C)** Alterations in miR-26a, miR-26b, and miR-141 in the cerebrospinal fluid of patients with PD and aged-matched healthy subjects (Con). $^{**}p < .01$ vs. vehicle; Student's *t* test. **(D)** The binding sites of miR-26a with DAPK1 3′ untranslated region (3′UTR) are conserved in mammalians. Hsa, human; Mmu, mouse; Rmk, Rhesus monkey; Rno, rat. **(E)** The wild-type (Wt) and mutant (Mut) 3′UTR of DAPK1 were subcloned into the psi-CHECK vector and transfected into HEK293 cells together with miR-26a mimics or its scrambled control. The luciferase intensity was measured. Unpaired Student's *t* test was used; $^{**}p < .01$ vs. the scrambled control-treated group; $n = 6$ for each group. **(F–H)** The N2a cells were treated with miR-26a mimics and its scrambled control or with A-miR-26a and its scrambled control for 24 hours. The cell lysates were collected for the detection of DAPK1 protein and messenger RNA expression. Representative blots **(F)**, quantitative analysis **(G)**, and the relative expression level of DAPK1 messenger RNA **(H)** are shown. $^{**}p < .01$ vs. the respective Con; $n = 6$; Student's *t* test. **(I)** Analysis of the correlation between the miR-26 level and DAPK1 protein levels in the brain tissue of chronic MPTP-injected mice. **(J)** A representative image of localization of miR-26 and DAPK1 in the dopaminergic neurons. Scale bar = 20 μm. DM1A, α-tubulin antibody; TH, tyrosine hydroxylase.

Patient Population and Cerebrospinal Fluid Collection

The PD group consisted of 28 patients with Hoehn and Yahr stage 1 PD (14) at the Department of Neurology, Union Hospital affiliated with Tongji Medical College (Wuhan, China). Patients with PD were diagnosed according to the United Kingdom Brain Bank criteria (15) and staged according to Hoehn and Yahr. The clinical diagnosis of idiopathic PD was established based on individual patients' medical history, physical examination, and laboratory results. The severity of motor symptoms was assessed in patients with PD using the Unified Parkinson's Disease Rating Scale part 3 (16). Cerebrospinal fluid (CSF) from the control group or the PD group was collected via routine lumbar puncture following confirmation of informed consent from each patient and/or a family member. Following centrifugation at 755*g* for 10 minutes, 3- to 4-mL CSF samples were aliquoted and stored at −80°C until analysis. Every CSF sample was tested by routine biochemical examination, and the results all were within the normal range. The information of PD and control brains for Western blot and immunohistochemistry studies are listed in Supplemental Table S4. The current study was approved by the Ethics Committee of Tongji Medical College.

Statistical Analysis

All data are shown as mean ± SD and were analyzed using SPSS version 16.0 (SPSS Inc., Chicago, IL). Normality was tested with Shapiro-Wilk test, and equal variance was evaluated before analysis of variance analysis. The difference between two groups was assessed using unpaired Student's *t* test (two tailed), and the variance among multiple groups was assessed by one- or two-way analysis of variance with/without repeated measures followed by Tukey, Dunnett, Newman-Keuls, or Bonferroni post hoc test, as indicated in the figure legends. The Mann-Whitney *U* test (two groups) and Kruskal-Wallis *H* test (three or more groups) were used for nonparametric testing. All experiments were repeated three times except those specified, and $p < .05$ was considered as statistically significant.

RESULTS

DAPK1 Is Increased in PD Mice and Is Positively Correlated With Synucleinopathy

To determine the possible role of DAPK1 in PD, we first examined the expression level of DAPK1 in the acute and chronic MPTP-injected mice. We found that in the SN of the acute MPTP-injected mice, the expression of DAPK1 was significantly increased compared with vehicle-treated control mice (Figure 1A). By using immunohistochemistry, we found that the enhanced staining of DAPK1 was mainly located in the cytoplasm of neurons (Figure 1B). In the chronic MPTP mouse model, DAPK1 protein expression was increased to approximately 2.3-fold of the control mice (Figure 1C, D), which was more apparent than the increase in the acute group. We also examined DAPK1 expression at different time points (1 month, 2 months, and 3 months) after MPTP injection in a chronic model and found that the elevation of DAPK1 protein peaked at 1 month (Supplemental Figure S1). These results show that DAPK1 is upregulated in the MPTP mouse model. Because the chronic MPTP mice displayed more obvious PD-like behavioral features and pathological changes (17) and apparent DAPK1 upregulation, we used the model of chronic MPTP administration for 1 month in the following experiments. We then examined the potential role of DAPK1 upregulation in the pathological changes, especially in neuronal synucleinopathy, in PD mice. By using double-immunofluorescence labeling with anti-DAPK1 and anti-phospho-Ser129-α-synuclein (anti-p-syn) or anti-α-synuclein (anti-t-syn) antibodies, we found that in the chronic MPTP mice the immunoreactivity of DAPK1, p-syn, and t-syn was much higher than that in the vehicle-treated mice. In particular, the neurons with stronger staining of DAPK1 also displayed enhanced immunosignals for p-syn and t-syn, and quantitative analysis suggests positive correlations between DAPK1 and p-syn and between DAPK1 and t-syn in the PD mouse model (Figure 1E–H). In addition, we found that the α-synuclein inclusions were more prominent in neurons with higher DAPK1 expression (Figure 1I). In addition, upregulation of DAPK1 was detected mainly in the DA neurons (Supplemental Figure S2). These findings suggest that DAPK1 upregulation is positively correlated with the progression DA neuron synucleinopathy in PD mice. We also examined the changes of DAKP1 in the SN of patients with PD. While Western blot and immunohistochemical analysis did not reveal any significant changes in the expression of DAPK1 between patients with PD and age-matched healthy control patients, Lewy bodies, the hallmark pathology of PD, were occasionally stained positive for DAPK1 (Supplemental Figure S3). Given that the extent of DAPK1 upregulation declined over time in the chronic MPTP mice (Supplemental Figure S1), and the PD samples were obtained from patients at their end stage of disease, these results likely suggest that upregulation of DAPK1 in the DA neurons occurred at the early stage of PD.

Reduction in miR-26a in the PD Model Induces DAPK1 Overexpression by Posttranscriptional Regulation

We next explored the mechanisms underlying DAPK1 upregulation in PD mice. We found that there was no difference in *Dapk1* mRNA levels in the acute and chronic MPTP mouse models (Figure 2A), suggesting that the upregulation of DAPK1 in PD mice is not caused by enhanced gene transcription. Recently, the posttranscriptional regulation of genes by miRNA has been well studied. We hypothesized that DAPK1 upregulation is mediated by the loss of specific miRNAs. We first analyzed the 3′ untranslated region (3′UTR) of the *Dapk1* gene via TargetScan7.0 and miRNA.org and found that miR-124, let-7/miR-98, miR-26a/b, and miR-141 were scored the highest in both predicted outputs (Supplemental Table S3). Using quantitative polymerase chain reaction, we examined alterations of those miRNAs in the SN of the chronic MPTP mice. We found that the levels of miR-141 and miR-26a/b were dramatically decreased, the level of let-7e was increased, while the other members of the let-7 family, miR-98 and miR-124, showed no change (Figure 2B). We further examined the levels of miR-141 and miR-26a/b in the CSF of patients with PD and found that only miR-26a was significantly decreased when compared with that of age-matched healthy subjects (Figure 2C). To verify the posttranscriptional regulation of DAPK1 by miR-26a, we constructed the wild-type (wt) 3′UTR of *Dapk1*, which contains the binding site to miR-26a, and a mutated version to the luciferase reporter vector, which were cotransfected into HEK293 cells with miR-26a mimics or a scrambled control (Figure 2D). We found that miR-26a mimics suppressed the luciferase activity in the wt constructs but not in the mutant constructs (Figure 2E). Moreover, overexpression of miR-26a reduced, whereas the miR-26a inhibitor elevated, DAPK1 protein expression in the N2a cells without changes in the *Dapk1* mRNA levels (Figure 2F–H). Importantly, although the 3′UTR of DAPK1 has two predicted binding sites for miR-141, none of them displayed significant responses in the luciferase experiment. Neither the mRNA nor the protein of DAPK1 was altered upon the treatment of miR-141 mimics, which further ruled out the potential regulation of DAPK1 by miR-141 (Supplemental Figure S4). miR-26a expression and DAPK1 protein expression displayed a negative correlation in the MPTP mice (Figure 2I). Furthermore, both the miR-26a transcript and the DAPK1 protein could be detected in the DA neurons of the SN (Figure 2J). These results suggest that miR-26a regulates DAPK1 expression at a posttranscriptional level in the DA neurons, and the loss of miR-26a mediates DAPK1 upregulation in PD mice.

A previous study identified that miR-26a transcription was positively regulated by the transcription factor C/EBPα (18); therefore, we examined the protein levels of C/EBPα in the SN of MPTP mice and found that it decreased to ∼40% of the level in the vehicle-treated mice (Supplemental Figure S5), indicating potential involvements of C/EBPα reduction in the loss of miR-26a in PD mice.

Loss of miR-26a or DAPK1 Upregulation Induces PD-like Pathological and Behavioral Changes

We then asked whether the dysfunction of the miR-26a/DAPK1 signaling pathway plays an important role in the pathogenesis of PD. We injected the miR-26a antagomir (A-miR-26a) or adeno-associated virus–packaged full-length mouse DAPK1 complementary DNA (AAV-DAPK1) into the SN of wt mice (Figure 3A). We found that both the A-miR-26a

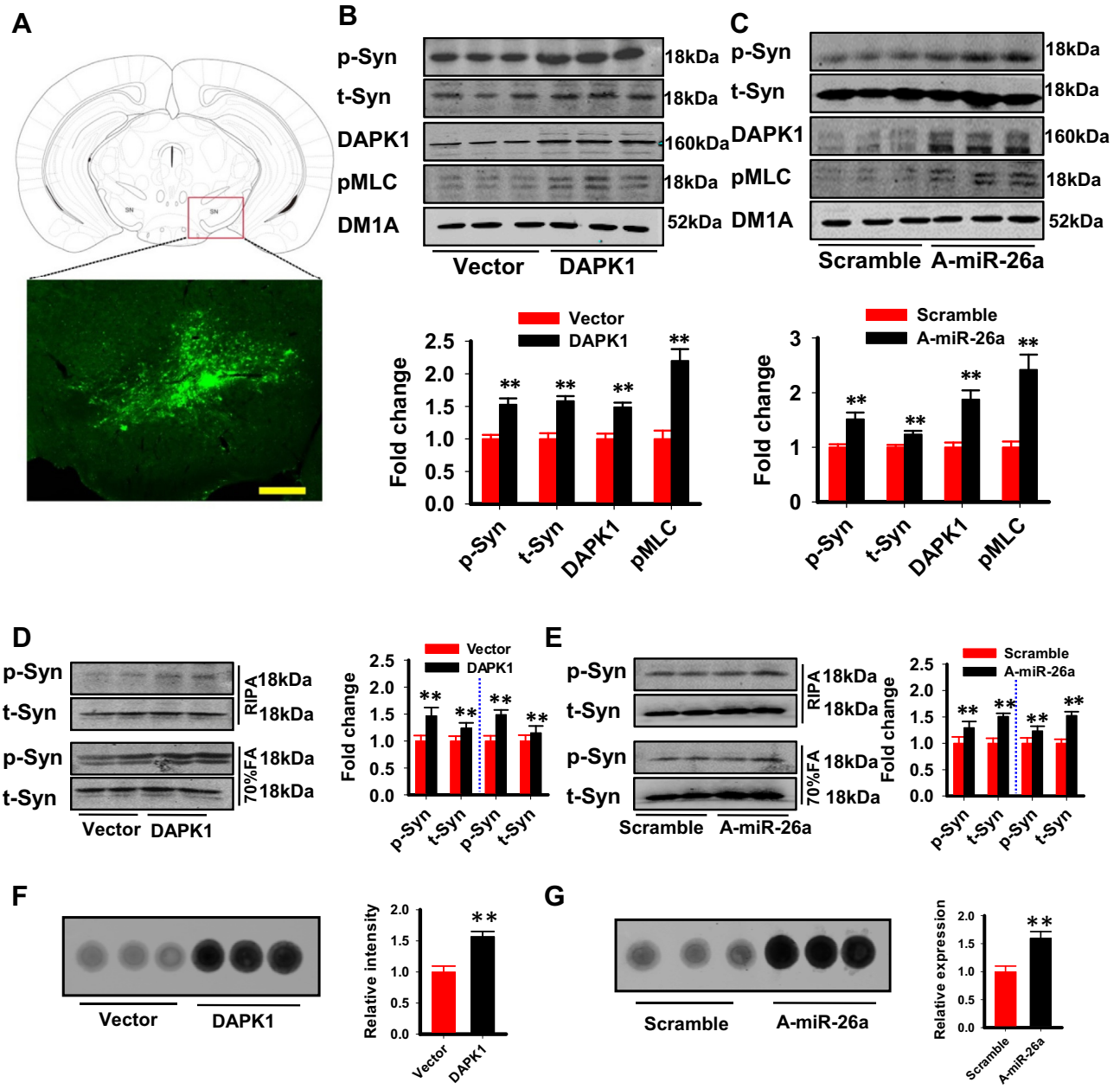

Figure 3. Overexpression of death-associated protein kinase 1 (DAPK1) or inhibition of microRNA-26a (miR-26a) induces synucleinopathy. **(A)** Diagram of the virus injection site (upper panel) and a representative fluorescence image (lower panel). **(B, C)** Effects of DAPK1 overexpression **(B)** and miR-26a inhibition **(C)** on the phosphorylation level and expression of α-synuclein in wild-type mice. The upper panels are representative blots, and the lower panels are the quantified data. A-miR-26a: miR-26a antagomir; DAPK1: AAV-DAPK1-IRES-EGFP virus; Scramble: the scrambled control for miR-26a antagomir; Vector: AAV-EGFP virus. $^{**}p < .01$ vs. vector **(B)** or scramble **(C)**; Student's *t* test; $n = 8$ from 3 independent experiments. **(D, E)** Effects of DAPK1 overexpression **(D)** and miR-26a inhibition **(E)** on the solubility of α-synuclein. The left panels are representative blots, and the right panels are the quantified data (left side of the blue dashed line for the 70% fatty acid [FA] and right side for the radioimmunoprecipitation assay [RIPA]). $^{**}p < .01$ vs. vector **(D)** or scramble **(E)**; Student's *t* test; $n = 8$ from 3 independent experiments. **(F, G)** The filter trap experiments were used to detect α-synuclein oligomer formation with DAPK1 overexpression **(F)** or miR-26a inhibition **(G)**. DM1A, α-tubulin antibody; pMLC, phosphorylation of myosin light chain; p-Syn, phospho-Ser129-α-synuclein; t-Syn, total α-synuclein.

treatment and the AAV-DAPK1 treatment led to not only activation of DAPK1 [indicated by the intensity of phosphorylation of myosin light chain according to previous studies (9)] but also hyperphosphorylation of α-synuclein at Ser129 and enhanced α-synuclein expression (Figure 3B, C). Because abnormally hyperphosphorylated α-synuclein usually aggregates to form insoluble fibrils in Lewy bodies, a dominant pathological change in PD, we examined the solubility of α-synuclein. We

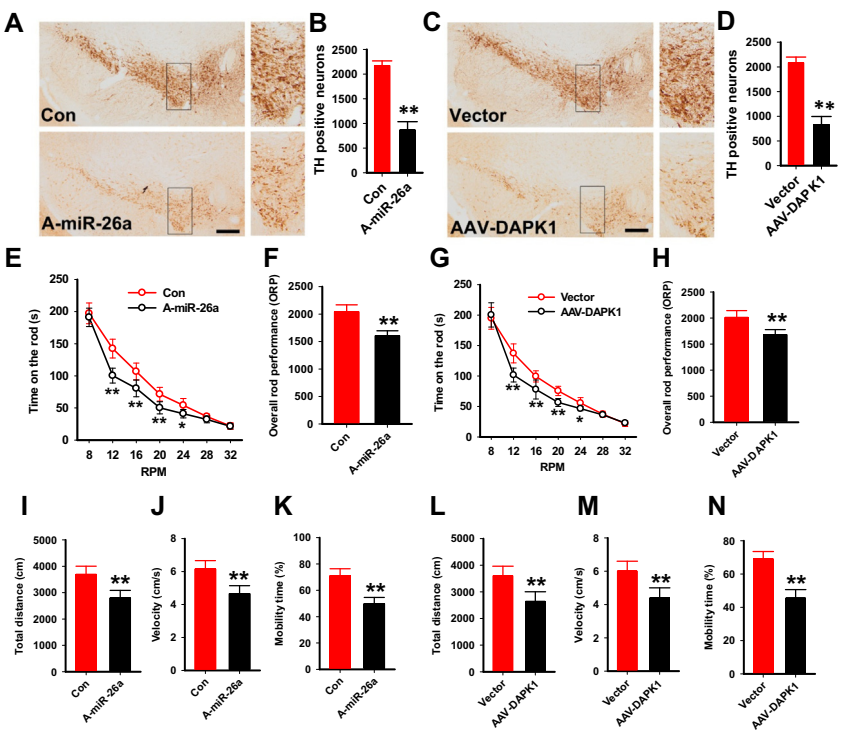

Figure 4. Overexpression of death-associated protein kinase 1 (DAPK1) or inhibition of microRNA-26a (miR-26a) induces dopaminergic neuron death and locomotor disabilities. **(A, B)** Immunohistochemistry of tyrosine hydroxylase (TH) staining in the substantia nigra of mice treated with miR-26a antagomir (A-miR-26a) or the scrambled control (Con). A representative image **(A)** and the quantification of TH-positive neurons **(B)** are shown. Bar = 100 μm; $^{**}p < .01$ vs. Con. **(C, D)** Immunohistochemistry of TH staining in the substantia nigra of mice treated with AAV-DAPK1 or the vector control. DAPK1: AAV-DAPK1-IRES-EGFP virus; Vector: AAV-EGFP virus. A representative image **(C)** and the quantification of TH-positive neurons **(D)** are shown. Bar = 100 μm; $^{**}p < .01$ vs. vector; Student's *t* test. **(E, F)** Mice were injected with A-miR-26a or the Con, and the rotarod test was performed. Time spent on the rod by mice in each group at different rotation speeds **(E)** and overall rotarod performance (ORP) scores in two groups **(F)** are shown. $^{**}p < .01$ vs. Con; $n = 10$; one-way analysis of variance with Bonferroni post hoc test was used. **(G, H)** Mice were injected with AAV-DAPK1 or the control virus (vector), and the rotarod test was performed. Time spent on the rod by mice in each group at different rotation speeds **(G)** and ORP scores in two groups **(H)** are shown. $^{**}p < .01$ vs. Con; $n = 10–11$; one-way analysis of variance with Bonferroni post hoc test was used. **(I–K)** The total distance traveled **(I)**, mean velocity **(J)**, and percentage of time spent mobile **(K)** in the open field test of mice treated with A-miR-26a or a control. $^{**}p < .01$ vs. Con; $n = 10$; Student's *t* test. **(L–N)** The total distance traveled **(L)**, mean velocity **(M)**, and percentage of time spent mobile **(N)** in the open field test of mice treated with AAV-DAPK1 or the control virus (vector). $^{**}p < .01$ vs. vector; $n = 10–11$; Student's *t* test. RPM, revolutions per minute.

found that the level of phosphorylated α-synuclein was dramatically increased in the radioimmunoprecipitation assay buffer fraction (soluble) and in the 70% fatty acid fraction (insoluble) (Figure 3D, E). Likewise, by using a filter trap assay, we found that α-synuclein oligomers were significantly increased in either miR-26a-inhibited or DAPK1-overexpressed mice (Figure 3F, G). These findings suggest that the loss of miR-26a or the upregulation of DAPK1 plays an important role in DA neuron synucleinopathy in PD mice.

Because α-synuclein aggregates are known to be cytotoxic, causing cell death of DA neurons in the SN and striatum of patients with PD, we then examined the loss of DA neurons by immunostaining with anti–tyrosine hydroxylase. We found that the total number of tyrosine hydroxylase–positive neurons in the SN was dramatically reduced in the A-miR-26a- and AAV-DAPK1-treated mice (Figure 4A–D). Because the loss of neurons in the SN is known to result in the motor symptoms in PD, we employed an open field arena test to observe spontaneous movements and a rotarod test to analyze motor coordination. In the rotarod tasks, the mice treated with A-miR-26a or AAV-DAPK1 demonstrated a significant decrease in the time spent on an accelerating rotarod and the overall rotarod performance compared with those outcomes in the control mice ($p < .05$) (19,20) (Figure 4E–H). This locomotor abnormality was also manifested in the open field experiments. The total distance traveled, mean velocity, and rearing time all were significantly decreased upon A-miR-26a or AAV-DAPK1 treatment (Figure 4I–N). These findings suggest that the loss of miR-26a or DAPK1 overexpression not only leads to DA neuron death but also causes impairments in locomotor functions.

Activation of DAPK1 Induces Synucleinopathy by Directly Phosphorylating α-Synuclein

We then wanted to determine whether DAPK1 activation promotes DA neuron synucleinopathy. Given the important role of DAPK1 in mediating autophagy (21), we first examined the degradation of α-synuclein. Cycloheximide chase analysis demonstrated that overexpression of DAPK1 did not extend the α-synuclein half-life (2 hours) compared with that of the pcDNA control (Addgene, Watertown, MA) (Figure 5A, B), excluding the potential involvement of protein degradation by DAPK1 activation. DAPK1 is a Ser/Thr kinase and phosphorylates multiple substrates under different pathological conditions, and the phosphorylation of α-synuclein is increased in mice exhibiting DAPK1 overexpression via miR-26a inhibition, AAV-DAPK1 infection, or MPTP treatment. Therefore, we hypothesized that DAPK1 could phosphorylate α-synuclein directly. We then transfected the wt DAPK1 plasmid or the wt α-synuclein vector into HEK293 cells and found that DAPK1 overexpression dramatically increased the levels of p-syn (Figure 5C). This effect is specific because mutating this Ser residue to alanine diminished the phosphorylation and the elevation in total α-synuclein (Figure 5D). Furthermore, we examined the temporal sequence of changes in phospho-synuclein and total synuclein. We found that upon the

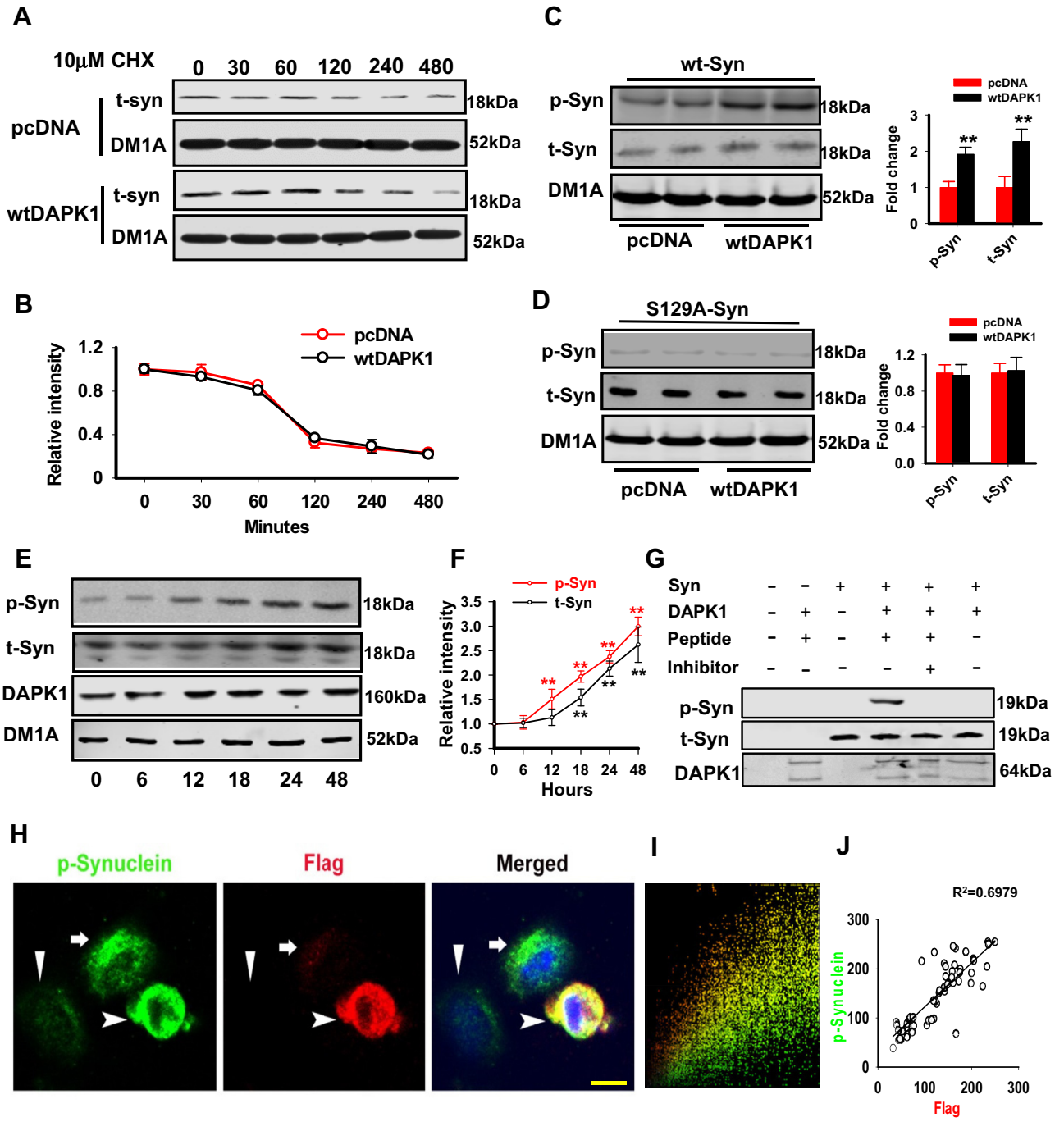

Figure 5. Death-associated protein kinase 1 (DAPK1) directly promotes the phosphorylation of α-synuclein at serine 129. **(A, B)** A representative Western blot image **(A)** of total α-synuclein protein levels during the cycloheximide (CHX) chase experiment. HEK293 cells were transfected with the wild-type (wt) α-synuclein plasmids with either wtDAPK1 or pcDNA. Then, 24 hours after transfection, cells were treated with CHX for the indicated time periods. Quantification of the data is shown **(B)**. $n = 3$ independent experiments; Student's t test. **(C, D)** HEK293 cells were cotransfected with the wt α-synuclein (wt-Syn) **(C)** or mutant (S129a-Syn) **(D)**, together with either wtDAPK1 or pcDNA. The cell lysates were collected 48 hours later for Western blotting. $^{**}p < .01$ vs. pcDNA; $n = 4$; Student's t test. **(E, F)** The N2a cells were transfected with wt DAPK1, and the cell lysates were collected at 0, 6, 12, 18, 24, and 48 hours for examination of pSer129-α-Synuclein (p-Syn) and total α-Synuclein (t-Syn). The representative blots **(E)** and the quantitative analysis **(F)** are shown. $^{**}p < .01$ vs. 0 hours; $n = 6$; Bonferroni post hoc test after repeated two-way analysis of variance. **(G)** The recombinant α-synuclein (human) and DAPK1 (human) were incubated in 30°C for 30 minutes, and the inhibitor at 69 nM was added, and these were then subjected to Western blot. The p-Syn, t-Syn, and DAPK1 were detected. **(H–J)** The N2a cells were transfected with Flag-DAPK1 plasmid and then double-immunostained with anti-p-Syn (green) and anti-DAPK1 (red) antibodies. The nuclei were visualized by 4′,6-diamidino-2-phenylindole staining **(H)**. A colocalization analysis **(I)** and a correlation analysis **(J)** were performed. Arrowhead: cell with higher DAPK1 level; arrow: cell with moderate DAPK1 expression; triangle: cell without DAPK1 expression. Scale bar = 10 μm. DM1A, α-tubulin antibody; p-Syn, phospho-Ser129-α-synuclein; t-Syn, total α-synuclein.

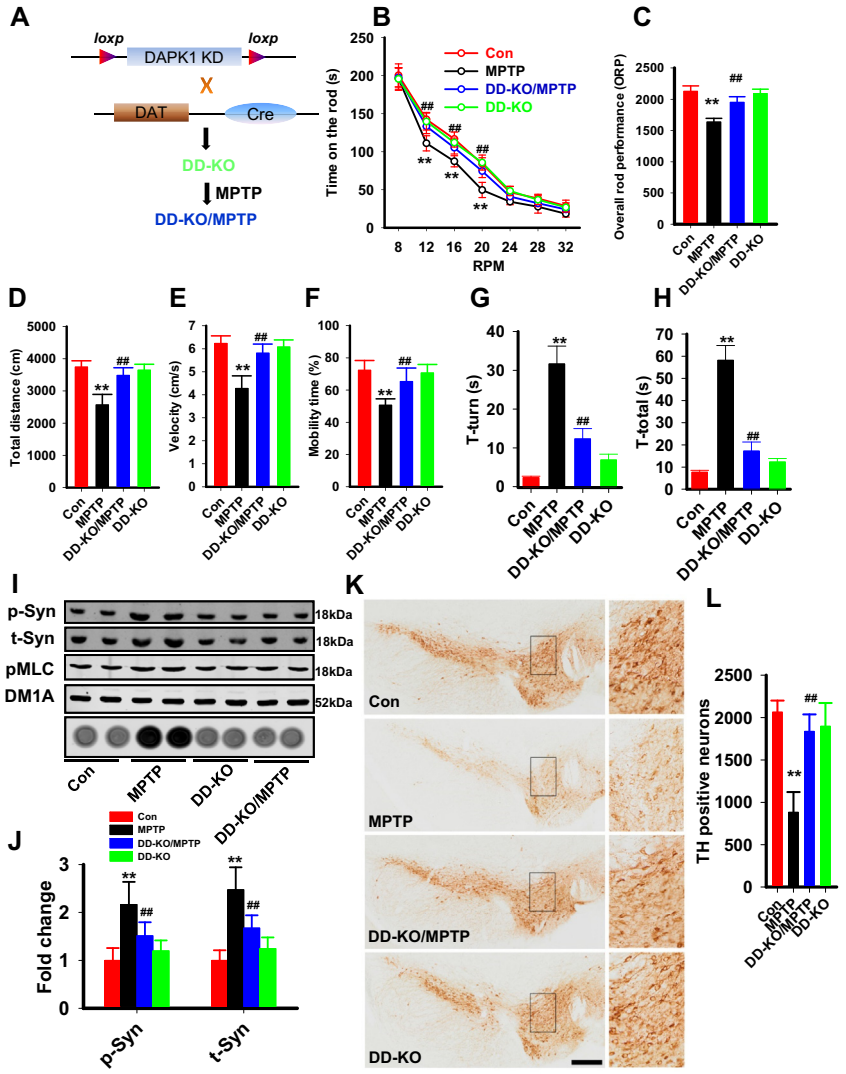

Figure 6. Genetic deletion of death-associated protein kinase 1 (DAPK1) rescues the Parkinson's disease–like behaviors and pathologies of 1-methyl-4-phenyl-1,2,3,6-tetrahydropyridine (MPTP) mice. **(A)** A diagram for the generation of DAPK1 knockout in dopamine neurons (DD-KO) mice and DD-KO/MPTP mice. **(B–H)** The wild-type mice (Con) and the DD-KO mice received a total of 10 doses of MPTP hydrochloride (25 mg/kg in saline, subcutaneous) on a 5-week schedule. The mice were then subjected to the rotarod test **(B, C)**, open field test **(D–F),** and pole test **(G, H)**. Time spent on the rod **(B)** and overall rotarod performance (ORP) **(C)** were measured. The total distance traveled **(D)**, mean velocity **(E)**, and mobility time **(F)** were evaluated in the open field test. The time to orient down (T-turn) **(G)** and total time to descend the pole (T-total) **(H)** were evaluated in the pole test. $^{**}p < .01$ vs. Con; $^{\#\#}p < .01$ vs. MPTP; one-way analysis of variance with Bonferroni post hoc test was used. **(I, J)** The mice were treated as described in **(B–H)**, and the homogenates from the substantia nigra were extracted for Western blotting (upper four blots) and the filter trap analysis (bottom dot blot). The representative blots **(I)** and the quantitative analysis for phospho-Ser129-α-synuclein (p-Syn) and total α-synuclein (t-Syn) **(J)** are shown. $^{**}p < .01$ vs. Con; $^{\#\#}p < .01$ vs. MPTP; $n = 6$; one-way analysis of variance with Bonferroni post hoc test was used. **(K, L)** Mice were treated as described in **(B–H)**, and the coronal slices from those mice were prepared for tyrosine hydroxylase (TH) staining. Representative images of the substantia nigra of different groups **(K)** and the quantitative analysis **(L)** are shown. $^{**}p < .01$ vs. Con; $^{\#\#}p < .01$ vs. MPTP; $n = 6$; one-way analysis of variance with Bonferroni post hoc test was used. DM1A, α-tubulin antibody; KD, kinase domain; pMLC, phosphorylation of myosin light chain; RPM, revolutions per minute.

DAPK1 overexpression, the increment in the phospho-Ser129 of α-synuclein began at 12 hours, but the increment of total α-synuclein began at 18 hours (Figure 5E, F), suggesting that DAPK1-induced α-synuclein phosphorylation occurred prior to the aggregation. In a cell-free system, coincubation of purified DAPK1 and α-synuclein protein for 30 minutes resulted in the hyperphosphorylation of α-synuclein at the Ser129 site. Application of TC-DAPK 6, a specific DAPK1 inhibitor, blocked the hyperphosphorylation of α-synuclein (Figure 5G). By using double-immunofluorescence staining, we verified the hyperphosphorylation of pS129-synuclein in wt DAPK1 plasmid–overexpressed cells (Figure 5H). The colocalization and correlation analysis indicated that the expression of DAPK1 was positively correlated with the phosphorylation levels of pS129-synuclein, suggesting a direct interaction of DAPK1 with α-synuclein (Figure 5I, J). These findings demonstrated that DAPK1 activation promotes DA neuron synucleinopathy via enhancing the phosphorylation of α-synuclein.

Genetic Deletion of DAPK1 in DA Neurons Rescues the PD-like Pathological and Behavioral Changes

We then wanted to know whether deletion of DAPK1 in DA neurons could rescue the PD-like pathological and behavioral changes in the chronic MPTP mice. We found that mice with DAPK1 knockout in the DA neurons (DD-KO/MPTP) displayed restored locomotor abilities in both of the rotarod tests (increased time on the rod and the overall rod performance), the open field tasks (restored total distance, velocity, and mobility time), and the pole test (shorter time to orient down and total time to descend the pole) (Figure 6A–H). Meanwhile, the enhanced phosphorylation and aggregation of α-synuclein was also attenuated in the SN of DD-KO/MPTP mice (Figure 6I, J). In the aged (18-month) A53T α-synuclein mutant mice, injection of lentivirus that contains the effective small interfering RNA for DAPK1 also repressed the hyperphosphorylation and aggregation of α-synuclein (Supplemental Figure S6). Furthermore,

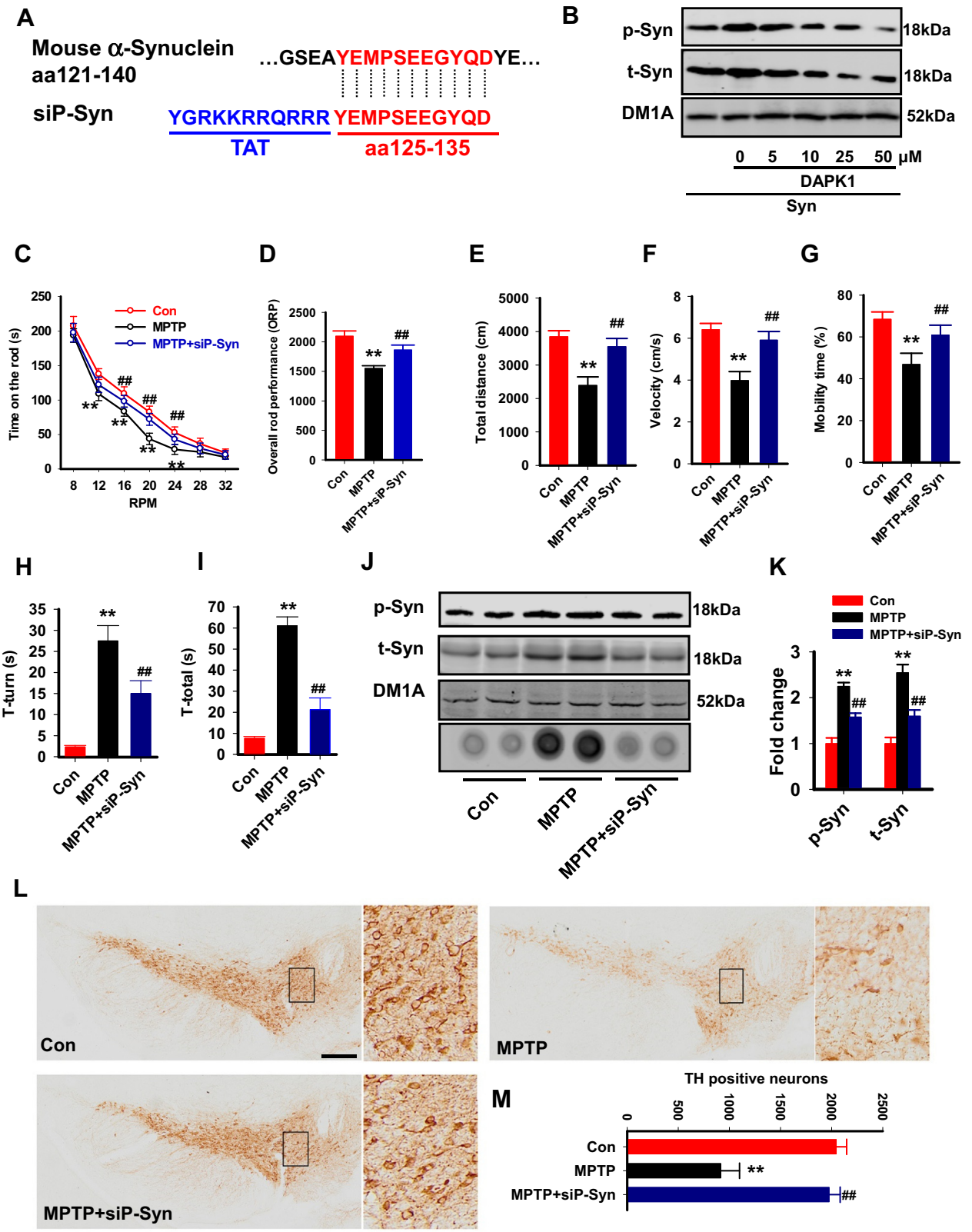
A
Mouse α-Synuclein aa121-140
…GSEAYEMPSEEGYQDYE…
siP-Syn
YGRKKRRQRRR
TAT
YEMPSEEGYQD
aa125-135
B
p-Syn
t-Syn
DM1A
18kDa
18kDa
52kDa
0 5 10 25 50 μM
DAPK1
Syn
C
Time on the rod (s)
RPM
Con
MPTP
MPTP+siP-Syn
D
Overall rod performance (ORP)
E
Total distance (cm)
F
Velocity (cm/s)
G
Mobility time (%)
H
T-turn (s)
I
T-total (s)
J
p-Syn
t-Syn
DM1A
18kDa
18kDa
52kDa
K
Fold change
L
Con
MPTP
MPTP+siP-Syn
M
TH positive neurons

deletion of DAPK1 reduced the loss of DA neurons in the SN (Figure 6K, L) induced by MPTP.

Beneficial Effects of the Phosphorylation Site of α-Synuclein Peptide in PD Mice

Finally, we disrupted the DAPK1 activation-induced hyperphosphorylation of α-synuclein by using a cell-permeable peptide and evaluated its effect on PD-like pathological and locomotor abnormalities. The peptide was generated by fusion of an HIV Tat (transactivator of transcription) signal (YGRKKRRQRRR) (22) to the competing peptide (23,24) that spans amino acids 125 to 135 (YEMPSEEGYQD) and contains the phosphorylation site (Ser129) of α-synuclein (siP-Syn) (Figure 7A). We first examined the phosphorylation of α-synuclein with different concentrations of siP-Syn peptide delivery to N2a cells. We found that application of 10 μM siP-Syn reduced the phosphorylation of α-synuclein as well as the aggregation of α-synuclein caused by DAPK1 overexpression in N2a cells (Figure 7B, C). We then injected siP-Syn once every 3 days at a dose of 10 mg/kg for 6 weeks. As expected, the siP-Syn peptide not only rescued the locomotor abnormalities in the MPTP mice (Figure 7D–H) but also reduced the hyperphosphorylation and aggregation of α-synuclein (Figure 7I, J). In addition, siP-Syn injection significantly promoted the survival of DA neurons in the brain (Figure 7K). Thus, blocking DAPK1-dependent phosphorylation of α-synuclein effectively rescues the PD-like pathological and behavioral changes.

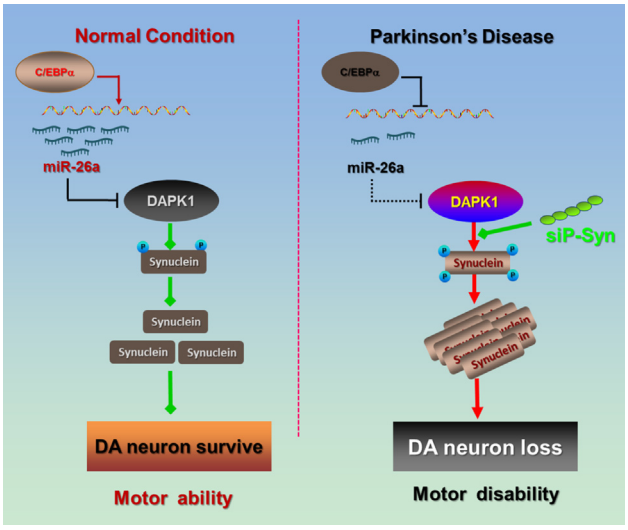

Figure 8. Schematic illustration of the effects of microRNA-26a (miR-26a). In the Parkinson's disease brain, the transcription factor CCAAT enhancer-binding protein alpha (C/EBPα) is suppressed and the transcription and expression of miR-26a are decreased. The loss of miR-26a induces posttranscriptional death-associated protein kinase 1 (DAPK1) overexpression, resulting in the hyperphosphorylation of α-synuclein and α-synuclein aggregation. The toxic synucleinopathy finally causes dopamine (DA) neuron death and locomotor disabilities in Parkinson's disease. siP-Syn, phosphorylation site (serine 129) of α-synuclein.

DISCUSSION

In the current study, we have reported that the DAPK1 protein is abnormally upregulated, a change that is positively correlated with DA neuron synucleinopathy in PD mice. We demonstrated that the loss of miR-26a caused by a reduction in the transcription factor C/EBPα in PD mice and patients with PD leads to an elevation in DAPK1 expression posttranscriptionally. We also revealed that both the loss of miR-26a and overexpression of DAPK1 induce α-synuclein hyperphosphorylation, aggregation, and inclusion formation, which further result in the death of DA neurons and locomotor abnormalities. Finally, by deleting DAPK1 in DA neurons or administering siP-Syn, a specific competing peptide, to MPTP mice, we found that neuronal synucleinopathy, DA neuron death, and the locomotor disabilities were dramatically attenuated or recovered. Thus, our study not only uncovered a novel role for miR-26a and DAPK1 in the pathological and behavioral abnormalities related to PD but also identified their potential application in the treatment for PD.

miRNAs are endogenous and short noncoding RNA molecules, 21 to 24 nucleotides in length, that play an important function in posttranscriptional regulation of gene expression through sequence-specific binding of the 3′UTR of target messenger RNA during neuronal development, differentiation, and maturation (25). Dysregulation of miRNAs has been implicated in the pathogenesis of multiple neurodegenerative diseases, including PD (26). As such, miR-7 and miR-153 have been shown to regulate α-synuclein levels synergistically, and depletion of these two miRNAs results in a concomitant increase in α-synuclein levels in a PD brain. Moreover, miR-7 has a protective role by preventing oxidative stress, and miR-7 inhibition causes cell death (27,28). In addition to miR-7 and miR-153, miR-26a has also been reported to be abnormally

Figure 7. The phosphorylation site (serine 129) of α-synuclein (siP-Syn) attenuates the behavioral and pathological abnormalities in Parkinson's disease mice. **(A)** A diagram of the siP-Syn design. Blue letters: Tat sequence. **(B)** The siP-Syn peptide blocked the phosphorylation of α-synuclein in vitro. The N2a cells were transfected with α-synuclein and death-associated protein kinase 1 (DAPK1), and the siP-Syn peptide was applied at different doses as indicated. Then, 24 hours later, the cell lysates were collected for Western blotting. **(C–I)** The siP-Syn peptide and its control (Con) peptide were injected into 1-methyl-4-phenyl-1,2,3,6-tetrahydropyridine (MPTP) mice, and the mice were subjected to the rotarod test, the open field test, and the pole test. The time on the rod **(C)** and overall rotarod performance (ORP) **(D)** were evaluated in the rotarod test. The total distance traveled **(E)**, mean velocity **(F)**, and mobility time **(G)** were evaluated in the open field test. The time to orient down (T-turn) **(H)** and total time to descend the pole (T-total) **(I)** were evaluated in the pole test. $^{**}p < .01$ vs. Con; $^{\#\#}p < .01$ vs. MPTP; $n = 9$, one-way analysis of variance with Bonferroni post hoc test was used. **(J, K)** The mice were treated as described in **(C–I)**, and the homogenates from the substantia nigra were extracted for Western blotting (upper three blots) and the filter trap analysis (lower dot blot). The representative blots **(J)** and the quantitative analysis for phospho-Ser129-α-synuclein (p-Syn) and total α-synuclein (t-Syn) **(K)** are shown. $^{**}p < .01$ vs. Con; $^{\#\#}p < .01$ vs. MPTP; $n = 6$; one-way analysis of variance with Bonferroni post hoc test was used. **(L, M)** The mice were treated as described in **(C–I)**, and the coronal slices from those mice were prepared for tyrosine hydroxylase (TH) staining. Representative images of the substantia nigra of different groups **(L)** and the quantitative analysis **(M)** are shown. $^{**}p < .01$ vs. Con; $^{\#\#}p < .01$ vs. MPTP; $n = 6$; one-way analysis of variance with Bonferroni post hoc test was used. aa, amino acids; DM1A, α-tubulin antibody; RPM, revolutions per minute.

downregulated in patients with PD (29) and PD cell lines (30). Here, we revealed that the expression of miR-26a was decreased both in the MPTP-induced PD mice and in the CSF of patients with PD. We also showed that the transcriptional factor C/EBPα, which was reported to control the transcription of miR-26a, was significantly reduced in the MPTP-treated mice. Therefore, we propose that the loss of C/EBPα causes a reduction in the transcription of miR-26a, leading to a reduced expression of miR-26a in PD. Furthermore, we found that miR-26a specifically binds to the 3′UTR of DAPK1 and represses DAPK1 translation. Inhibition of miR-26a expression in vivo resulted in synucleinopathy and DA neuron loss as well as locomotor disabilities, whereas an increase in miR-26a effectively ameliorates those abnormalities in PD mice. These findings strongly suggest a critical role for miR-26a in the pathological and behavioral changes in PD.

As an important mediator of cell death in response to ceramide, ischemia, and glutamate toxicity, DAPK1 is implicated in the pathogenesis of multiple neurological diseases such as epilepsy, AD, and ischemic brain injury. In AD, overexpression of DAPK1 promotes tau phosphorylation at multiple AD-related sites and increases its stability (11). In addition, DAPK1 activation enhances tau phosphorylation at Ser262 and results in tau insolubility and accumulation in dendritic spines, leading to synaptic dysfunction in ischemic stroke (31). Here, we have reported that activated DAPK1 in PD promotes the phosphorylation of α-synuclein at the Ser129, a site related to the neurotoxicity of α-synuclein. In Lewy bodies, a key pathological hallmark in PD brains, approximately 90% of α-synuclein is hyperphosphorylated at Ser129 (32). In both *Drosophila* and rat PD models (33,34), p-syn has been well studied for its participation in neuronal toxicity, especially in DA neuronal death. In this study, the phosphorylation level of p-syn was enhanced by DAPK1, resulting in the loss of DA neurons in the SN region. Thus, reduction in the phosphorylation level of p-syn could be a potential therapeutic approach for alleviating the pathological changes in PD. To this end, we generated the DD-KO mice to inhibit DAPK1-induced α-synuclein hyperphosphorylation and demonstrated that both strategies mitigate the previously observed synucleinopathy and DA neuron death as well as locomotor disabilities. Moreover, intravenous delivery of a membrane-permeable competing peptide also attenuated the synucleinopathy pathology and locomotor abnormalities. As one of the cell-penetrating peptides, Tat has been used to introduce multiple neuroprotective proteins to reduce cerebral ischemic damage and protect against ischemia in brain injury (35). In addition to the application in animal models, cell-penetrating peptide–mediated drug delivery has also been clinically investigated. For example, KAI-9803, a specific inhibitor of δPKC, and KAI-1678, a specific inhibitor of εPKC, were fused with Tat. These reagents exhibited acceptable safety and tolerability profiles (36) and were under phase II clinical trials for myocardial infarction and pain, respectively. Therefore, the competing peptide used in this study may provide a possible treatment strategy for PD.

Overall, our study demonstrates an important role of the miR-26a/DAPK1 signaling pathway in neuronal synucleinopathy, DA neuron loss, and locomotor disability in PD (Figure 8). Findings from this work indicate novel therapeutic targets and treatment strategies for PD.

ACKNOWLEDGMENTS AND DISCLOSURES

This work was supported partially by the National Natural Science Foundation of China (Grant Nos. 81761138043, 81829002, 91632114, 81771150, and 31571039 [to L-QZ], Grant No. 31721002 [to YL], Grant No. 81871108 [to DL], and Grant No. 81400897 [to YS]), the National Natural Science Foundation of China–U.S. National Institutes of Health joint program (Grant No. 81361120404 [to BT]), Key Project of National Science Foundation of China (Grant No. 81430023 [to BT]), National Program for Support of Top-Notch Young Professionals and Academic Frontier Youth Team of Huazhong University of Science and Technology (to LQ-Z), Program for Changjiang Scholars and Innovative Research Team in University (Grant No. IRT13016 [to J-GC]), and the U.S.-China Program for Biomedical Collaborative Research of National Institute of Neurological Disorders and Stroke (Grant No. NS083498 [to XZ]). Some brain tissues were obtained from the NIH NeuroBioBank.

L-QZ and DL initiated, designed, and supervised the study. YS, M-FD, WX, and A-JX performed the molecular biological experiments and animal experiments. YS, Z-HL, and BH collected the CSF samples of patients with PD. J-GC, BT, H-YM, and YL gave some comments and participated in the discussion for this manuscript. YS, M-FD, WX, and L-QZ analyzed the data. L-QZ and H-YM wrote the manuscript.

The peptide used to block synuclein phosphorylation was submitted to the Patent Office of the People's Republic of China by L-QZ, M-FD, DL, A-JX, and Ya-Fan Zhou (Application No. 2018100396990). All other authors report no biomedical financial interests or potential conflicts of interest.

ARTICLE INFORMATION

From the Department of Neurology (YS, Z-HL, BH), Union Hospital, Department of Pathophysiology (M-FD, WX, A-JX, L-QZ), Key Lab of Neurological Disorder of Education Ministry, Department of Medical Genetics (DL), School of Basic Medicine, Tongji Medical College, and Institute of Brain Research (YS, M-FD, WX, A-JX, J-GC, YL, DL, L-QZ), Collaborative Innovation Center for Brain Science, Huazhong University of Science and Technology, Wuhan, and National Research Center for Geriatric Diseases (JG, BT, L-QZ), Xiangya Hospital, and Center for Medical Genetics, School of Life Science, Central South University, Changsha, Hunan, China; Department of Pathology (XZ), Case Western Reserve University, Cleveland, Ohio, and Department of Biology (H-YM), Boston University, Boston, Massachusetts.

YS, M-FD, and WX contributed equally to this work.

Address correspondence to Ling-Qiang Zhu, Ph.D., Department of Pathophysiology, Key Lab of Neurological Disorder of Education Ministry, School of Basic Medicine, Tongji Medical College, Huazhong University of Science and Technology, Wuhan 430030, China; E-mail: zhulq@mail.hust.edu.cn; or Beisha Tang, Ph.D., National Research Center for Geriatric Diseases, Xiangya Hospital, and Center for Medical Genetics, School of Life Science, Central South University, 87 Xiangya Road, Changsha 410008, Hunan, China; E-mail: bstang7398@163.com.

Received Jul 23, 2018; revised Dec 6, 2018; accepted Dec 7, 2018.

Supplementary material cited in this article is available online at https://doi.org/10.1016/j.biopsych.2018.12.008.

REFERENCES

1. GBD 2015 Mortality and Causes of Death Collaborators (2016): Global, regional, and national life expectancy, all-cause mortality, and cause-specific mortality for 249 causes of death, 1980-2015: A systematic analysis for the Global Burden of Disease Study 2015. Lancet 388:1459–1544.
2. Xia R, Mao ZH (2012): Progression of motor symptoms in Parkinson's disease. Neurosci Bull 28:39–48.
3. Michel PP, Hirsch EC, Hunot S (2016): Understanding dopaminergic cell death pathways in Parkinson disease. Neuron 90:675–691.
4. Dexter DT, Jenner P (2013): Parkinson disease: From pathology to molecular disease mechanisms. Free Radic Biol Med 62:132–144.
5. Bialik S, Kimchi A (2006): The death-associated protein kinases: Structure, function, and beyond. Annu Rev Biochem 75:189–210.

6. Deiss LP, Feinstein E, Berissi H, Cohen O, Kimchi A (1995): Identification of a novel serine/threonine kinase and a novel 15-kD protein as potential mediators of the gamma interferon-induced cell death. Genes Dev 9:15–30.
7. Shohat G, Spivak-Kroizman T, Cohen O, Bialik S, Shani G, Berrisi H, *et al.* (2001): The pro-apoptotic function of death-associated protein kinase is controlled by a unique inhibitory autophosphorylation-based mechanism. J Biol Chem 276:47460–47467.
8. Inbal B, Bialik S, Sabanay I, Shani G, Kimchi A (2002): DAP kinase and DRP-1 mediate membrane blebbing and the formation of autophagic vesicles during programmed cell death. J Cell Biol 157:455–468.
9. Tu W, Xu X, Peng L, Zhong X, Zhang W, Soundarapandian MM, *et al.* (2010): DAPK1 interaction with NMDA receptor NR2B subunits mediates brain damage in stroke. Cell 140:222–234.
10. Pei L, Shang Y, Jin H, Wang S, Wei N, Yan H, *et al.* (2014): DAPK1–p53 interaction converges necrotic and apoptotic pathways of ischemic neuronal death. J Neurosci 34:6546–6556.
11. Kim BM, You MH, Chen CH, Lee S, Hong Y, Hong Y, *et al.* (2014): Death-associated protein kinase 1 has a critical role in aberrant tau protein regulation and function. Cell Death Dis 5:e1237.
12. Wang X, Liu D, Huang HZ, Wang ZH, Hou TY, Yang X, *et al.* (2018): A novel microRNA-124/PTPN1 signal pathway mediates synaptic and memory deficits in Alzheimer's disease. Biol Psychiatry 83:395–405.
13. Sambandan S, Akbalik G, Kochen L, Rinne J, Kahlstatt J, Glock C, *et al.* (2017): Activity-dependent spatially localized miRNA maturation in neuronal dendrites. Science 355:634–637.
14. Hoehn MM, Yahr MD (2001): Parkinsonism: Onset, progression, and mortality. 1967. Neurology 57(10 Suppl 3):S11–S26.
15. Hughes AJ, Daniel SE, Kilford L, Lees AJ (1992): Accuracy of clinical diagnosis of idiopathic Parkinson's disease: A clinico-pathological study of 100 cases. J Neurol Neurosurg Psychiatry 55:181–184.
16. Goetz CG, Tilley BC, Shaftman SR, Stebbins GT, Fahn S, Martinez-Martin P, *et al.* (2008): Movement Disorder Society-sponsored revision of the Unified Parkinson's Disease Rating Scale (MDS-UPDRS): Scale presentation and clinimetric testing results. Mov Disord 23: 2129–2170.
17. Petroske E, Meredith GE, Callen S, Totterdell S, Lau YS (2001): Mouse model of Parkinsonism: A comparison between subacute MPTP and chronic MPTP/probenecid treatment. Neuroscience 106:589–601.
18. Mohamed JS, Lopez MA, Boriek AM (2010): Mechanical stretch upregulates microRNA-26a and induces human airway smooth muscle hypertrophy by suppressing glycogen synthase kinase-3 beta. J Biol Chem 285:29336–29347.
19. Rozas G, Guerra MJ, Labandeira-Garcia JL (1997): An automated rotarod method for quantitative drug-free evaluation of overall motor deficits in rat models of parkinsonism. Brain Res Brain Res Protoc 2:75–84.
20. Rozas G, Lopez-Martin E, Guerra MJ, Labandeira-Garcia JL (1998): The overall rod performance test in the MPTP-treated-mouse model of Parkinsonism. J Neurosci Methods 83:165–175.
21. Zalckvar E, Berissi H, Eisenstein M, Kimchi A (2009): Phosphorylation of Beclin 1 by DAP-kinase promotes autophagy by weakening its interactions with Bcl-2 and Bcl-XL. Autophagy 5:720–722.
22. Bechara C, Sagan S (2013): Cell-penetrating peptides: 20 years later, where do we stand? FEBS Lett 587:1693–1702.
23. Moles A, Sanchez AM, Banks PS, Murphy LB, Luli S, Borthwick L, *et al.* (2013): Inhibition of RelA-Ser536 phosphorylation by a competing peptide reduces mouse liver fibrosis without blocking the innate immune response. Hepatology 57:817–828.
24. Oakley F, Teoh V, Ching ASG, Bataller R, Colmenero J, Jonsson JR, *et al.* (2009): Angiotensin II activates I kappaB kinase phosphorylation of RelA at Ser 536 to promote myofibroblast survival and liver fibrosis. Gastroenterology 136:2334–2344.
25. O'Carroll D, Schaefer A (2013): General principals of miRNA biogenesis and regulation in the brain. Neuropsychopharmacology 38:39–54.
26. Hoss AG, Labadorf A, Beach TG, Latourelle JC, Myers RH (2016): MicroRNA profiles in Parkinson's disease prefrontal cortex. Front Aging Neurosci 8:36.
27. Junn E, Lee KW, Jeong BS, Chan TW, Im JY, Mouradian MM (2009): Repression of alpha-synuclein expression and toxicity by microRNA-7. Proc Natl Acad Sci U S A 106:13052–13057.
28. Doxakis E (2010): Post-transcriptional regulation of alpha-synuclein expression by mir-7 and mir-153. J Biol Chem 285:12726–12734.
29. Martins M, Rosa A, Guedes LC, Fonseca BV, Gotovac K, Violante S, *et al.* (2011): Convergence of miRNA expression profiling, alpha-synuclein interacton and GWAS in Parkinson's disease. PLoS One 6:e25443.
30. Li L, Chen H, Chen F, Li F, Wang M, Wang L, *et al.* (2013): Effects of glial cell line-derived neurotrophic factor on microRNA expression in a 6-hydroxydopamine-injured dopaminergic cell line. J Neural Transm (Vienna) 120:1511–1523.
31. Pei L, Wang S, Jin H, Bi L, Wei N, Yan H, *et al.* (2015): A novel mechanism of spine damages in stroke via DAPK1 and tau. Cereb Cortex 25:4559–4571.
32. Schlossmacher MG, Frosch MP, Gai WP, Medina M, Sharma N, Forno L, *et al.* (2002): Parkin localizes to the Lewy bodies of Parkinson disease and dementia with Lewy bodies. Am J Pathol 160:1655–1667.
33. Chen L, Feany MB (2005): Alpha-synuclein phosphorylation controls neurotoxicity and inclusion formation in a *Drosophila* model of Parkinson disease. Nat Neurosci 8:657–663.
34. Yamada M, Iwatsubo T, Mizuno Y, Mochizuki H (2004): Overexpression of alpha-synuclein in rat substantia nigra results in loss of dopaminergic neurons, phosphorylation of alpha-synuclein and activation of caspase-9: Resemblance to pathogenetic changes in Parkinson's disease. J Neurochem 91:451–461.
35. Zou LL, Ma JL, Wang T, Yang TB, Liu CB (2013): Cell-penetrating peptide-mediated therapeutic molecule delivery into the central nervous system. Curr Neuropharmacol 11:197–208.
36. Guidotti G, Brambilla L, Rossi D (2017): Cell-penetrating peptides: From basic research to clinics. Trends Pharmacol Sci 38:406–424.